Flores, P., Modeling and simulation of wear in revolute clearance joints in multibody systems. Mechanism and Machine Theory, Volume 44, Issue 6, June 2009, Pages 1211-1222. (http://dx.doi.org/10.1016/j.mechmachtheory.2008.08.003,)

Departamento de Engenharia Mecânica, Universidade do Minho,
Campus de Azurém, 4800-058 Guimarães Portugal
Phone: + 351 253510220; Fax: + 351 253516007; E-mail: pflores@dem.uminho.pt

Abstract

The main goal of this work is to develop a methodology for studying and quantifying the wear phenomenon in revolute clearance joints. In the process, a simple model for a revolute joint in the framework of multibody systems formulation is presented. The evaluation of the contact forces developed is based on a continuous contact force model that accounts for the geometrical and materials properties of the colliding bodies. The friction effects due to the contact in the joints are also represented. Then, these contact-impact forces are used to compute the pressure field at the contact zone, which ultimately is employed to quantify the wear developed and caused by the relative sliding motion. In this work, the Archard's wear model is used. A simple planar multibody mechanical system is used to perform numerical simulations, in order to discuss the assumptions and procedures adopted throughout this work. From the main results obtained, it can be drawn that the wear phenomenon is not uniformly distributed around the joint surface, owing to the fact that the contact between the joint elements is wider and more frequent is some specific regions.

Keywords: Wear, Clearance joints, Contact-Impact, Multibody dynamics

1. Introduction

It is well known that most of the common mechanical systems include contact and relative motion between the bodies which, among other phenomena, can be a source of wear. According to standard DIN 50320, wear can be defined as "the progressive loss of material from the surface of a solid body due to mechanical action, i.e., the contact and relative motion against a solid, liquid or gaseous counter body" [1]. In other words, wear is quantified by the loss of material from contacting surfaces when they are subjected to a relative motion.

The large amount and variety of works and models have been presented over the last decades show how wear in mechanical systems is of paramount importance [2, 3]. Wear is a quite complex phenomenon that takes place when two or more bodies contact each other, involving a wide variety of parameters, such as geometry of contact, temperature of contact, physical and chemical properties of the contacting materials, thus playing a crucial role in many engineering areas such as machine design and tribology. The wear phenomenon is a topic rather difficult to be understood, especially if all the possible physical and chemical influence parameters are taken into account. Thus, the selection of the adequate materials and suitable design methodologies are desired in order to achieve optimized wear.

Figure 1 depicts an example of a surface failure caused by fatigue, owing to the clearance joint impacts. Figure 1a shows a connecting rod of a motorcycle internal combustion engine in which the connection with the piston was made with an unlubricated needle bearing. Figure 1b shows a lubricated pin used in a motorcar internal combustion engine. In both cases, the surface failure was caused by the shear stress, occurred a short distance below surface, due to the dynamic loads which, after several thousands of cycles, lead to the fatigue failure of the components. This type of surface failure is characterized by fatigue cracks which progress into and under the surface, and particles that tear out of the surface. The craters resulting from this process are known as pits or spalls [4]. These two surface failure examples clearly demonstrate the importance of considering the effect of the clearance on impact behavior, and its influence on the wear system, in the design stage of the components.

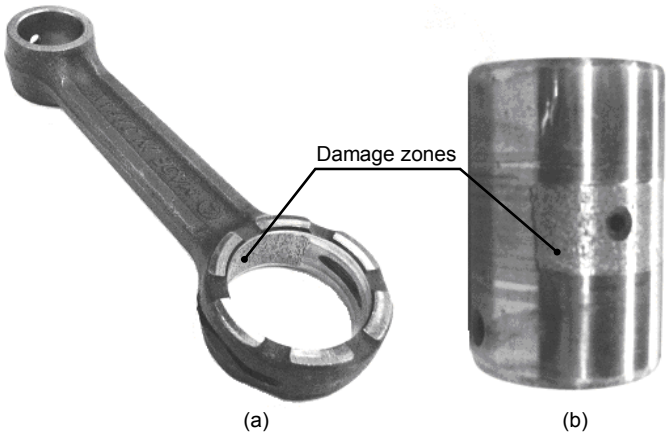

Figure 1: Failure components: (a) Connecting rod; (b) Pin.

The finite element method (FEM) is one of the most popular methods for modeling and simulating the wear process due to its accuracy and also owing to its ability to deal with complex contact geometries [5, 6]. However, from computational point of view, the FEM is very time consuming. Thus, a quite interesting alternative, in a designer point of view, is the use of more straightforward approaches based on the contact conditions and materials properties, which can easily be integrated in a general code for dynamics of mechanical systems. These formulations, besides their popularity, present a very good accuracy and numerical efficiency [7, 8].

There are two main approaches to model the wear in mechanical contacts, namely the Reye's hypothesis [9] and the Archard's wear model [10]. The Reye's hypothesis tells that, in the case of dry friction, the volume of removed material is proportional to work performed by the friction forces. Tasora et al. [7] used the Reye's hypothesis to record the amount of work of the friction force in polar coordinates. They quantify, both theoretically and experimentally, the surface wear on a revolute joint, and global results agree quite well. Furthermore, they observed that the wear does not affect the entire surface of the shaft, but mostly happened on specific spots. Pennestri et al. [11] also based on the Reye's hypothesis, estimated the wear of a cam follower mechanism actuated robotized gearbox, in order to improve the design of the cam profile by achieving uniform wear.

As for as the Archard's wear model is concerned, it correlates the wear volume with some physical and geometrical properties of the sliding bodies, such as applied load, sliding distance and hardness. The Archard's approach is, in fact, the most popular and widely used model to predict the wear in gear and cam-follower mechanisms [12-14]. Jourdan [15] also used the Archard's equation to numerically simulate the wear in a knee joint prosthesis. The Archard's wear equation represents a macroscopic model, since the microscopic effects like asperities deformations and material tearing are not directly taken into account. These effects are considered through a macroscopic wear coefficient. Furthermore, the temperature effects can be neglected, based on the assumption that the relative sliding velocity remains at low levels and the applied load does not exceed a limit where seizure takes place. In these circumstances, the wear that occurs is characterized as delaminating wear, which arises from the adhesive forces set up whenever atoms come into intimate contact. In delaminating wear, the sliding velocity is low enough to allow for surface heating to be neglected [16]. The Archard's model describes this wear mechanism.

The main purpose of this work is to investigate the wear process between two contacting bodies, under the framework of a general formulation for multibody mechanical systems involving joints surface interaction. With this approach it can be possible to predict how a worn surface will affect the wear, as well as to access data on desired tribological behavior for mating surfaces, thus prolonging the life of mechanical components and their performance. The problem is dealt with in two dimensions, therefore, the multidirectional effects are not taken into account.

2. Equations of motion of multibody systems

When the configuration of a multibody is described by *n* Cartesian coordinates $\mathbf{q}$, then a set of *m* algebraic kinematic independent constraints $\mathbf{\Phi}$ can be written as [17],

$$\mathbf{\Phi}(\mathbf{q}, t) = \mathbf{0} \tag{1}$$

Differentiating Eq. (1) with respect to time yields the velocity constraint equation. After a second differentiation with respect to time the acceleration constraint equation is obtained as follows,

$$\mathbf{\Phi}_{\mathbf{q}}\dot{\mathbf{q}} = \boldsymbol{\upsilon} \tag{2}$$

$$\mathbf{\Phi}_{\mathbf{q}}\ddot{\mathbf{q}} = \boldsymbol{\gamma} \tag{3}$$

where $\mathbf{\Phi}_{\mathbf{q}}$ is the Jacobian matrix of the constraint equations, $\boldsymbol{\upsilon}$ is the right side of velocity equations, and $\boldsymbol{\gamma}$ is the right side of acceleration equations, which contains the terms that are exclusively function of velocity, position and time.

The equations of motion for a constrained multibody mechanical system can be written as [18],

$$\mathbf{M}\ddot{\mathbf{q}} = \mathbf{g} + \mathbf{g}^{(\mathbf{c})} \tag{4}$$

in which where $\mathbf{M}$ is the system mass matrix, $\ddot{\mathbf{q}}$ is the vector that contains the state accelerations, $\mathbf{g}$ is the generalized force vector, which contains all external forces and moments, and $\mathbf{g}^{(\mathbf{c})}$ is the vector of constraint reaction equations.

The joint reaction forces can be expressed in terms of the Jacobian matrix of the constraint equations and the vector of Lagrange multipliers as [18],

$$\mathbf{g}^{(\mathbf{c})} = -\mathbf{\Phi}_{\mathbf{q}}^{\mathrm{T}}\boldsymbol{\lambda} \tag{5}$$

where $\boldsymbol{\lambda}$ is the vector that contains *m* unknown Lagrange multipliers associated with *m* holonomic constraints. Substitution of Eq. (5) in Eq. (4) yields,

$$\mathbf{M}\ddot{\mathbf{q}} + \mathbf{\Phi}_{\mathbf{q}}^{\mathrm{T}}\boldsymbol{\lambda} = \mathbf{g} \tag{6}$$

In dynamic analysis, a unique solution is obtained when the constraint equations are considered simultaneously with the differential equations of motion with proper set of initial conditions [17]. Therefore, Eq. (3) is appended to Eq. (6), yielding a system of differential algebraic equations that are solved for $\ddot{\mathbf{q}}$ and $\boldsymbol{\lambda}$. This system is given by,

$$\begin{bmatrix} \mathbf{M} & \boldsymbol{\Phi}_{\mathbf{q}}^{\mathrm{T}} \\ \boldsymbol{\Phi}_{\mathbf{q}} & \mathbf{0} \end{bmatrix} \begin{Bmatrix} \ddot{\mathbf{q}} \\ \boldsymbol{\lambda} \end{Bmatrix} = \begin{Bmatrix} \mathbf{g} \\ \boldsymbol{\gamma} \end{Bmatrix} \tag{7}$$

In each integration time step, the accelerations vector, $\ddot{\mathbf{q}}$, together with velocities vector, $\dot{\mathbf{q}}$, are integrated in order to obtain the system velocities and positions at the next time step. This procedure is repeated up to final time will be reached.

The set of differential algebraic equations of motion (7) does not use explicitly the position and velocity equations associated with the kinematic constraints, Eqs. (1) and (2), respectively. Consequently, for moderate or long time simulations, the original constraint equations are rapidly violated due to the integration process. Thus, in order to stabilize or keep under control the constraints violation, Eq. (7) is solved by using the Baumgarte stabilization method [19] and the integration process is performed using a predictor corrector algorithm with variable step and order [20].

3. Numerical wear models

Meng and Ludema [3] referred that there are more than 300 approaches for wear and friction phenomena. Most of these models include parameters and constants that are valid only for some specific cases. Nevertheless, very few of those wear models have been used to predict wear in everyday engineering design [12]. In a broad sense, there are two main approaches to predict wear that are commonly used in tribology, namely the Reye's hypothesis [9] and the Archard's equation [10]. These two models correlate the wear volume with some physical and geometrical properties of the contacting bodies, such as applied load, sliding distance and hardness, among others.

The Reye's hypothesis, also known as energy dissipative hypothesis, states that the volume of removed material is proportional to the work done by the tangential friction force, and can be written as,

$$\frac{V}{s} = \frac{F_T}{\tau} \qquad (8)$$

where V is the wear volume, s represents the sliding distance, F_T is the tangential friction force and τ is a constant that characterizes the shear stress of the sliding bodies. Assuming that the volume of worn material is equal to the product of the contact area by the thickness of the worn material, then the Reye's hypothesis can be re-written as follows,

$$\frac{dh}{ds} = \frac{\mu p}{\tau} \qquad (9)$$

in which μ is the friction coefficient, p is the contact pressure and the remaining parameters are the same as defined above.

As far as the Archard's wear approach is concerned, it should be highlighted that this linear wear model was firstly proposed by Holm [21], although it has been usually named as Archard's wear equation. This model was developed and based on experimental tests and can be expressed by [10],

$$\frac{V}{s} = \frac{KF_N}{H} \qquad (10)$$

where V is the wear volume, s is the sliding distance, K is the dimensionless wear coefficient, F_N represents the normal contact force and H is the hardness of the softer material.

The wear coefficient, which depends on the material properties, is introduced in this wear model to ensure agreement between theoretical and experimental results. Holm [21] considered this coefficient as a constant representing the number of abraded atoms per atomic accounter [22]. Assuming that the asperities of the surface, in the contact area, deform in a plastic manner and the actual contact area is proportional to the normal applied force, Archard [10] generalized the Eq. (10) as,

$$\frac{V}{s} = KA_a = \frac{KF_N}{H} \qquad (11)$$

in which, A_a is the actual contact area and the remaining parameters are as defined previously. Dividing Eq. (11) by A_a results in,

$$\frac{h}{s} = \frac{Kp}{H} \qquad (12)$$

Equation (12) represents the wear depth, which is more convenient for engineering applications than wear volume. The wear depth is related to the contact pressure distribution and, as bodies lose material, this distribution changes as the contact area changes with respect to the sliding distance.

Considering that the ratio h/s represents the wear rate at any time, then the Eq. (12) can be rewritten as,

$$\frac{dh}{ds} = \frac{Kp}{H} \qquad (13)$$

which looks quite similar to Eq. (9) for the Reye's hypothesis, and where K is the dimensionless wear coefficient, p represents the contact pressure and H is the hardness of the softer material.

Since, the wear process can be understood as a dynamic problem, which can be analyzed as an initial value problem thus, using for instance the Euler integration algorithm, the wear given by Eq. (13) can be integrated over the sliding distance, yielding,

$$h_{j+1} = h_j + \Delta h_j \qquad (14)$$

in which h_{j+1} is the total wear up to the j+1th wear step, h_j is the total wear up to the jth wear step and Δh_j is the amount of wear for the j+1 wear step, i.e., for the current wear step.

4. Formulation of revolute clearance joints

Figure 2 shows the typical configuration of a revolute joint with clearance. The joint elements are the bearing and journal, which radii are R_B and R_J, respectively. The difference between the bearing and journal radii is the radial clearance, c. The clearance in realistic joints is much smaller than the size of the bodies; however, in Fig. 2 is exaggerated for illustration purpose. The existence of the clearance in the revolute joints allows two extra degrees of freedom, that is, the horizontal and vertical displacement and, consequently, the journal and bearing can freely move relative to each other. In addition, Fig. 2 shows the relative penetration or indentation between the journal and bearing when the two bodies impact to each other.

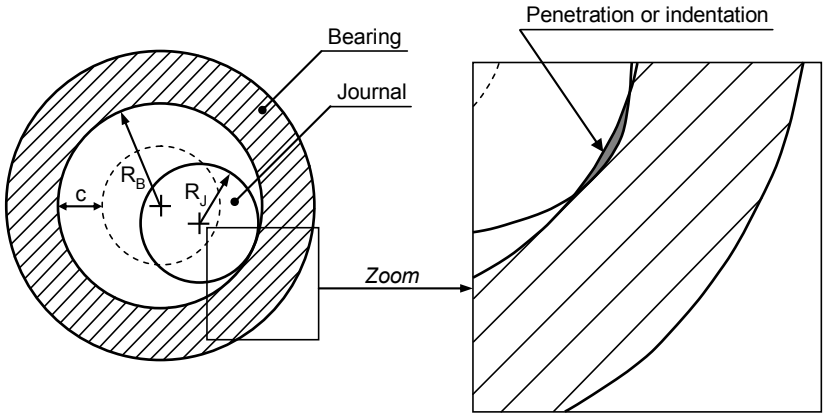

Figure 2: Revolute joint with clearance.

Figure 3 shows normal and tangential force components due to the impact between the journal and the bearing. The impact which has both normal and tangential relative velocities is treated as an eccentric oblique collision between two bodies.

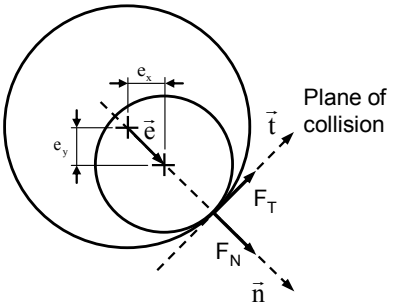

Figure 3: Normal and tangential forces that act between the journal and bearing in consequence of an impact.

From configuration of the system, the relative penetration depth between the journal and the bearing can be defined as,

$$\delta = e_{BJ} - c \qquad (15)$$

where e_{BJ} is the magnitude of the eccentricity vector defined between the bearing and journal center, and c is the radial clearance, which is a specified parameter.

The dynamics of a dry journal-bearing is characterized by two different situations. Firstly, when the journal and bearing are not in contact each other, there is no contact forces associated with the journal-bearing. Secondly, when the contact between the two bodies takes place, the contact-impact forces are modeled according to a nonlinear Hertz force law [23] together with the Coulomb friction law [24]. These conditions can be expressed as,

$$\mathrm{F} = 0 \qquad (\textit{if there is no contact}) \tag{16}$$

$$\mathrm{F} = \mathrm{F_N} + \mathrm{F_T} \qquad (\textit{if there is contact}) \tag{17}$$

where F_N and F_T are normal and tangential force components represented in Fig. 3. The direction of the forces is consistent with their application on the bearing. The interested reader on the details of the modeling of revolute joints with clearance is referred to references [25, 26].

The normal and tangential forces are given by,

$$\mathrm{F_N} = \mathrm{K_g}\delta^{\mathrm{n}} + \mathrm{D}\dot{\delta} \tag{18}$$

$$\mathrm{F_T} = -\mathrm{c_f c_d F_N}\frac{\mathbf{v}_\mathrm{T}}{\left\|\mathbf{v}_\mathrm{T}\right\|} \tag{19}$$

in which K_g is the generalized stiffness constant and δ is the relative penetration depth, n is the nonlinear exponent, D is the damping factor, $\dot{\delta}$ is the penetration velocity, c_f is the friction coefficient, $\mathbf{v}_T$ is the relative tangential velocity and c_d is a dynamic correction coefficient [23, 24].

The disadvantage when using a friction model such as the one represented by Eq. (19), for simulation or control purpose, is the problem of detecting when the relative tangential velocity is zero. A solution for this problem is found in the model proposed by Karnopp, which was developed to overcome the problems with zero velocity detection and to avoid switching between different state equations for sticking and sliding [27]. The drawback with this model is that it is so strongly coupled with the rest of system. The external force is an input to the model and this force is not always explicitly given. Variations of the Karnopp model are widely used since they allow efficient simulations, such as the modified Karnopp model by Centea et al. [28] and the reset integrator model by Haessig and Friedland [29]. In fact, the presence of friction in the contact surfaces makes the contact problem more complicated as the friction may lead to different modes, such as sticking or sliding. For instance, when the relative tangential velocity of two impacting bodies approaches zero, stiction occurs. Indeed, as pointed out by Ahmed et al. [30], the friction model must be capable of detecting sliding, sticking and reverse sliding to avoid energy gains during impact. This work was developed for the treatment of impact

problems in jointed open loop multibody systems. Lankarani [31] extends Ahmed formulation to the analysis of impact problems with friction in any general multibody system including both open and closed loop systems.

In simulating the dynamics of mechanical systems with clearance joints, it is essential to determine the instant of contact between the bodies that constitute the joints. The coupling of the relatively slow motion of the overall system with the faster motion, associated with the joint clearance parameters, makes the *eigenvalues* of the matrix of coefficients and independent terms of the equations of motion widely spread. Hence, numerical algorithms with variable step size and order are an important feature for the computational strategy [20, 32, 33]. The use of these numerical schemes plays a key role in contact problems, whose dynamic response is quite complex and discontinuous, due to the sudden change in kinematic structure caused by rapid variation of the contact forces applied to the system and to the dramatic change in the system stiffness, when a contact condition is achieved. Thus, before the first impact, the joint elements can freely move relative to each other and, in this phase, the step size is relatively large and the global configuration of the system is characterized by large translational and rotational displacements. Therefore, the first impact between the colliding bodies is often made with a high penetration depth, and, consequently, the contact forces are large too. This forces the integration process to go back and take a smaller step size, until a step can be taken which is within the given error tolerance [34]. The journal is considered in free flight motion relative to the bearing until the geometric equality criterion of Eq. (15) is verified, and, consequently, the contact between the journal and bearing wall is initialized. Ideally, when $\delta=e_{BJ}-c=0$, the bearing and the journal are in contact to each other. However, due to the computation round-off errors accumulation, a tolerance is introduced in order to accommodate for inaccuracies in the numerical results. In the present work, the bearing and journal are considered to be in contact when the penetration depth is larger than 1.0×10^{-10}m. Therefore, when the 'first' penetration is within the penetration tolerance it is assumed that such is the moment of the impact and the position and relative velocity of the contact points and the direction of the plane of collision are recorded. It should be highlighted that with this methodology, the step size can reach smaller values than those needed to keep the integration tolerance error under control. When the step size goes below the limit, it is forced to remain at the minimum value [34, 35].

5. Modeling wear in revolute clearance joints

In the present work, the Archard's wear model is used to predict the amount of wear in a revolute joint with clearance. This type of joint is commonly found in almost all mechanical systems. In a simple way, a revolute joint with clearance is modeled as two contacting bodies, as illustrated in Fig. 2. According to the revolute joint clearance model presented in the previous section, in a dry contact situation the journal can move freely within the bearing until contact between the two bodies takes place. The contact, which has both normal and tangential relative velocities, is treated as an eccentric oblique collision between two bodies. When the journal impacts the bearing wall, a normal contact force coupled with a friction law is evaluated to obtain the dynamics of the journal-bearing. These forces are of a complex nature, and their corresponding impulse is transmitted throughout the mechanical system. The way normal and friction forces are modeled is of paramount importance in the dynamics of mechanical systems, since these forces directly influence the over all system's response [35]. On the other hand, contact conditions, leading to severe wear, can dramatically affect the performance of the mechanical systems. For sticking conditions, the wear is null, since there is no relative motion between the two contacting bodies.

According to this approach, being the contact forces developed between the journal and bearing known, the amount of wear depth produced can be estimated using Eq. (13). In order to compute the exact area covered by sliding distance, the joint surface is divided into several sectors before starting the simulation and, then, the wear depth in each sector is evaluated.

Figure 4 shows how the journal surface is divided into sectors. In each integration time step, when the contact between the journal and bearing occurs, the wear depth calculated for each sector is stored. At the end of simulation, the amount of wear depth accumulated on a sector is the sum of all partial wear depths at each time step. This approach, that is used to quantify the wear depth, is commonly referred as an incremental method. With this methodology, it is possible to compute the new geometric configuration of the joint surface caused by wear.

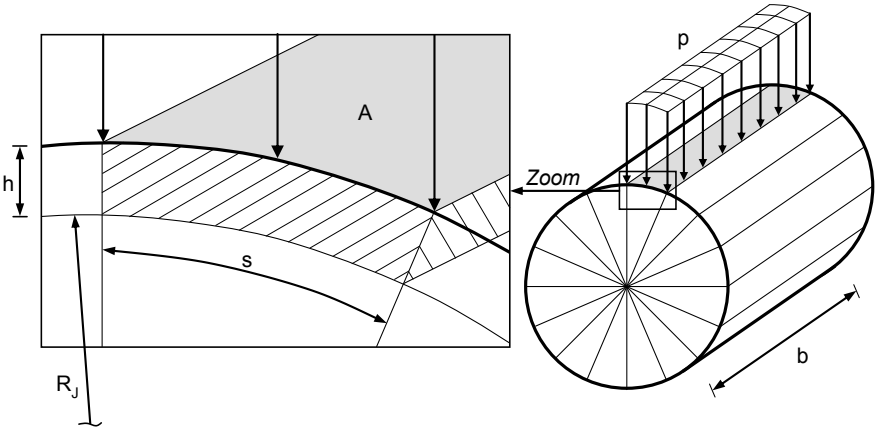

A – Nominal contact area [m^2] h – Wear depth [m] R_J – Nominal journal radius [m]
b – Journal-bearing width [m] p – Contact pressure [Pa] s – Sliding distance [m]

Figure 4: Journal surface divided into several sectors to perform the wear. The amount of wear of the sector selected is exaggerated for illustration.

The total amount of wear depth can be expressed by,

$$h = \sum h_i \qquad (20)$$

where *i* represents the number of sector in which the joint surface is divided. Based on the revolute joint geometric properties, the new journal and bearing radii at each time step are given by,

$$R_J^* = R_J - h/2 \qquad (21)$$

$$R_B^* = R_B + h/2 \qquad (22)$$

where R_J and R_B are, respectively, the nominal or initial journal and bearing radii and h is the total amount of wear depth along the joint surface, given by Eq. (20). These new values are evaluated at each time step and for each joint sector.

It is assumed that the total amount of wear is uniformly distributed between the journal and the bearing, that is, the wear depth in the journal is equal to the wear depth in the bearing, being this valued evaluated as half of the total wear depth.

Since the evaluation of the wear involves a good deal of both mathematical and computational manipulation, it is convenient to summarize the main steps in an appropriate algorithm. This algorithm, presented in the flowchart of Fig. 5, is developed in the framework of the multibody methodology and can be condensed in the following steps:

i) Start at instant of time t^0, with given initial conditions for positions $\mathbf{q}^0$ and velocities $\dot{\mathbf{q}}^0$.

ii) Define joint and material properties (R_B, R_J, K and i).

iii) Check for contact between the journal and bearing surfaces: if there is contact, determine the normal and tangential contact forces according to constitutive laws; otherwise, proceed normally with multibody formulation.

iv) Evaluate the pressure field developed at the sectors in which there is contact.

v) Compute the amount of wear depth in each sector at the current time step.

vi) Add the wear of each sector to the total wear worn out in the previous times steps.

vii) Determine the new journal and bearing radii.

viii) Apply a multibody formulation in order to obtain the new generalized positions and velocities of the system for time step $t+\Delta t$.

ix) Update the system time variable. Go to step iii) and proceed with the whole process for the new time step, until the final time for the analysis is reached.

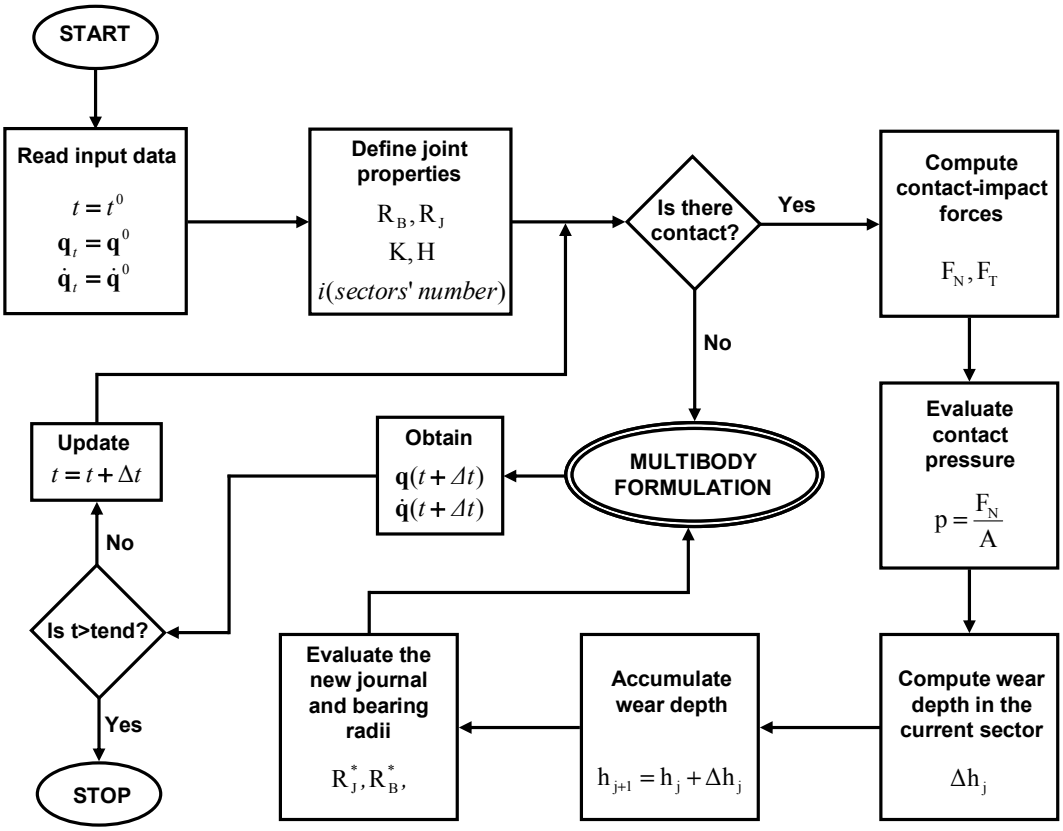

Figure 5 Flowchart of the algorithm proposed to model wear in the framework of multibody systems formulation.

6. Demonstrative application to a four bar mechanism

In this section an elementary four bar mechanism is used to show how the consideration of clearance in a revolute joint can affect its behavior, as well as to demonstrate the effect of the introduction of the wear phenomenon quantification. The four bar mechanism consists of four rigid bodies that represent the ground, crank, coupler and follower. The body numbers and their corresponding local coordinate systems are shown in Fig 6. The joints of this mechanism include three ideal revolute joints connecting the ground to the crank, the crank to the coupler and the ground to the follower. A single revolute joint with clearance was considered in the linkage between the coupler and follower. Figure 6 shows three frames from an animation sequence, where clearance was strongly exaggerated in order to clearly demonstrate the bouncing effect introduced in the dynamics.

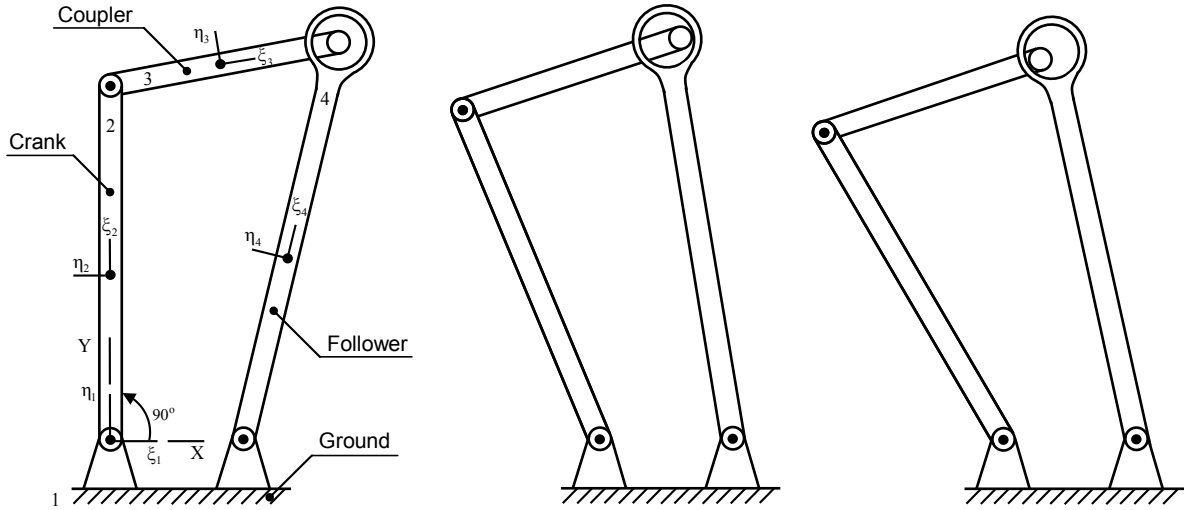

Figure 6: Four bar mechanism with a revolute joint clearance between the coupler and follower. The left-most picture corresponds to the initial simulation configuration.

The dimensions and inertia properties of each body are presented in Table 1. The dynamic parameters, used for the simulation and for the numerical methods required to solve the system dynamics, are listed in Table 2.

Body Nr.	Length [m]	Mass [Kg]	Moment of inertia [Kgm^2]
1	0.150	-	-
2	0.400	3.120	0.042
3	0.260	2.028	0.012
4	0.460	3.588	0.064

Table 1: Geometric and inertia properties of the four bar mechanism.

Bearing radius	10.0 mm
Journal radius	9.8 mm
Journal-bearing width	20.0 mm
Restitution coefficient	0.9
Friction coefficient	0.1
Young's module	207 GPa
Poisson's ratio	0.3
Wear coefficient	8×10^{-14} Pa^{-1}

Table 2: Parameters used in the dynamic simulation of the four bar mechanism.

In order to initiate the numerical simulation a set of initial conditions is required, bearing in mind that these can play a crucial role in the prediction of the dynamical response of the mechanical systems. The initial conditions used here are based upon the results of a kinematic analysis of the four bar mechanism in which all the joints are assumed to be ideal or perfect. The subsequent initial conditions for each time step in the simulation are obtained from the final conditions of the previous time step. This process is performed until the final time of analysis is reached. The crank is the driving link and rotates at a constant angular velocity of 50π rad/s.

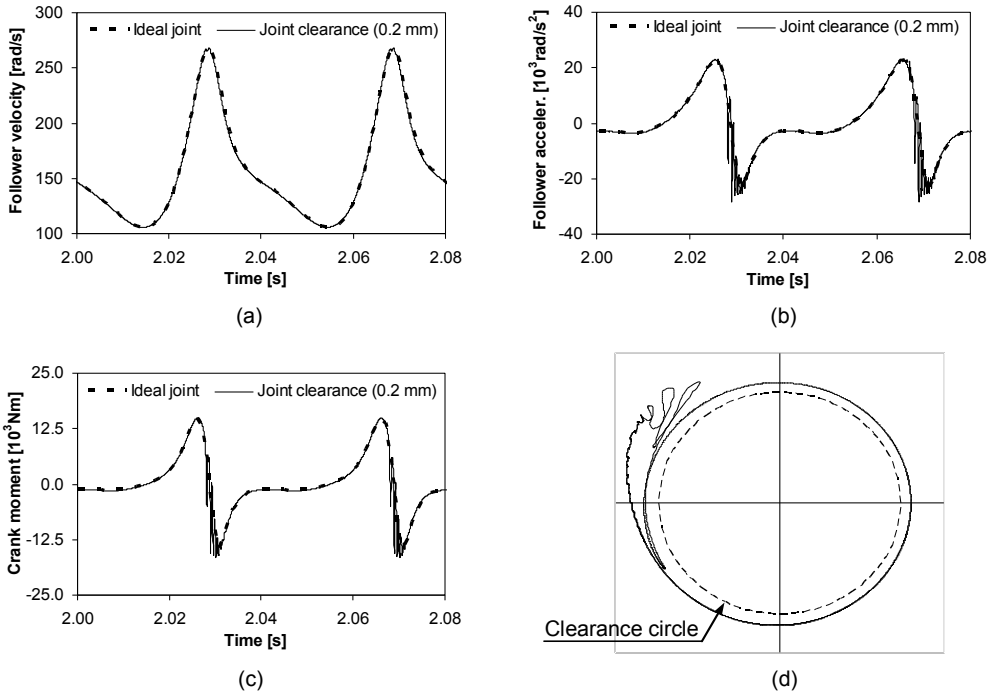

Figure 7 (a) Follower angular velocity; (b) Follower angular acceleration; (c) Crank moment required to maintain the crank angular velocity constant; (d) Journal centre orbit relative to the bearing center.

Prior to access the results concerning to the wear effect, a long time simulation was performed, in order to understand joint clearance influence in the global dynamics of the four bar mechanism. For this stage, two different kinds of results are here presented and discussed. Firstly, the four bar mechanism was modeled considering all joints as ideal, with neither clearance nor friction and a perfect alignment of journal and bearing rotating axes. Secondly, the mechanism was simulated with a revolute joint clearance, leading to surface contact phenomena in that links. The dynamic response of the four bar mechanism is represented in Figs. 7a and 7b by the time plots of the velocity and acceleration of the follower. The moment acting on the crank, required to maintain constant crank angular velocity, is plotted in Fig. 7c. The relative motion between the journal and bearing centers is also plotted in Fig. 7d. The Hertz contact force law with hysteretic damping factor [23] is used to evaluate the contact force between the journal and bearing. In

addition, the Coulomb friction conditions are assumed to exist at the contact [24]. It should be noted that the results are plotted against those obtained for the ideal joint, being reported for two full crank rotations after steady-state has been reached.

In general, the angular velocity of the follower is affected by the existence of the joint clearance but it is not discernable from the ideal values, as illustrated in Fig. 7a. Indeed, there is no deviation in the follower velocity curve when the four bar mechanism is simulated with both the ideal and the clearance joints. In sharp contrast to the follower angular velocity, the angular acceleration of the follower presents significant differences between the dynamic response of the four bar mechanism, when modeled with and without joint clearance. Upon reviewing Fig. 7b, it is clear that the acceleration peaks are directly related to the contact between the journal and bearing, during the simulation. These peaks are propagated throughout the rigid bodies until the crank moment diagram, in which some deviation from the ideal curve is also visible, as shown in Fig. 7c. Furthermore, the system's response clearly repeats itself from cycle to cycle. From Fig. 7d it is evident that the journal is always in contact with the bearing wall. This behavior can be expected, as the two bodies are moving in the same direction.

The global results obtained here are comparable to those published in the available literature, namely in what concerns the nonlinear nature response of mechanical systems when modeled with clearance joints. In a similar manner as it is pointed out in this study, Dubowsky and Freudenstein [36, 37] observed that the presence of clearance in the joints results in amplification in the internal dynamic system's forces. This work was subsequently extended by Dubowsky and Gardner [38] to include the elasticity of links. Dubowsky [39] showed how clearances can interact dynamically with machine control systems to destabilize and produce undesirable limit cycle behavior. Other researchers also included the influence of the bodies' flexibility in the dynamic performance of mechanical systems besides the existence of gaps in the joints [40, 41]. Dubowsky and Moening [42] obtained a reduction in the impact force level by introducing bodies' flexibility. They also observed a significant reduction of the acoustical noise produced by the impacts when the system incorporates bodies' flexible.

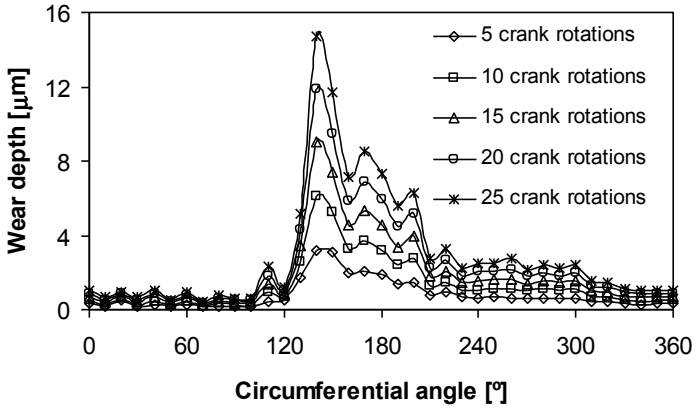

Figure 8: Journal surface wear depth accumulated for 5, 10, 15, 20 and 25 full crank rotations.

As far as the wear is concerned, it must be highlighted that the wear coefficient used to perform the numerical simulations was selected upon the best published data [14]. Here, and for simulations purposes only, the smaller values for the wear coefficient were applied, in order to accelerate the wear phenomenon. Furthermore, the considerably high clearance size used also increases contact forces and, consequently, the wear.

Figure 8 shows the wear depth accumulated for 5, 10, 15, 20 and 25 full crank rotations. The joint surface is divided in to 36 sectors. The wear depth is plotted against the circumferential angle, which defines the direction of contact between the journal and bearing. It is well visible that the wear phenomenon does not affect in the same manner the entire joint surface, but mostly the wear occurs on specific regions or sectors. The wear is much more accentuated in the range 140-200º of the circumferential angle. This observation is supported by the fact that the contact between the journal surface and bearing wall is wider and more frequent in the sectors corresponding to this angular range. The total amount of wear accumulated in all sectors during the simulation is also illustrated in Fig. 9, which corresponds to one second of simulation. Again, it is evident the non uniformity of the wear around the joint surface.

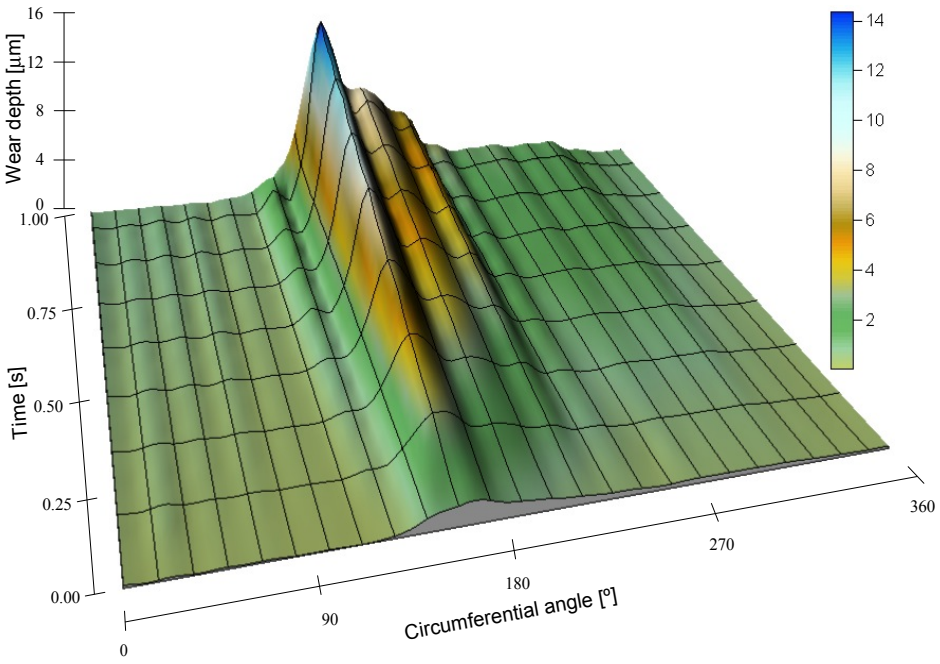

Figure 9: Journal surface accumulated wear depth for the first second of simulation.

The effect of the wear depth on the journal surface is illustrated in Fig. 10, where the initial and final geometric configurations are compared. As it was expected, the final configuration is not regular due to the non uniform wear produced around the journal surface. It worth noting that, in the present work, it was assumed that the wear is equally distributed between the journal and bearing.

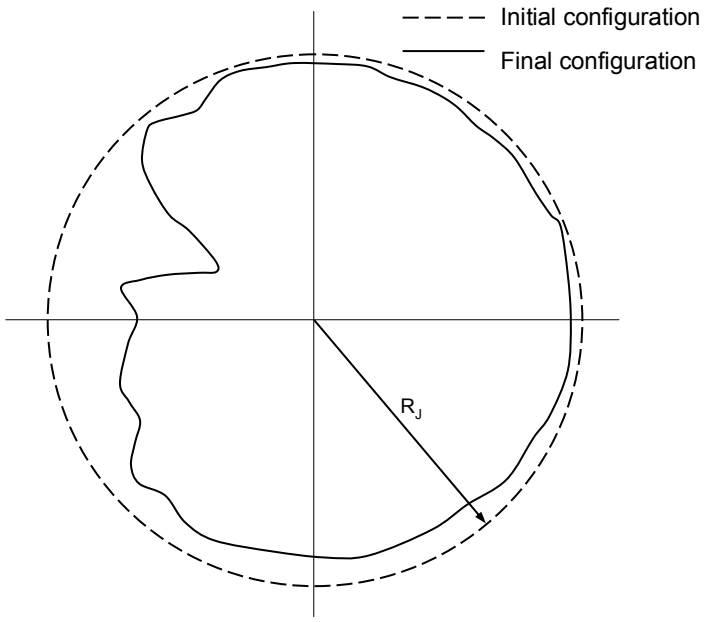

Figure 10: Initial and final journal geometry. The final configuration is not regular due to non uniform wear.

7. Concluding remarks

A general methodology for modeling and evaluating wear in mechanical systems has been presented in this work. This approach is developed under the framework of a multibody systems formulation. The wear model used is based on the generalized Archard's equation, which relates the volume of material loss with physical and geometrical properties of the contacting bodies. This wear approach is quite easy and straightforward to implement in a computational program. An elementary four bar mechanism, which includes a revolute joint with clearance, was used as a numerical example application, to show the wear phenomenon and its global dynamics behavior. From the main qualitative and quantitative results obtained, it was demonstrated that the wear depth along the joint surface is non uniform, due to the fact that the contact between the journal and bearing walls is wider and more frequent is some specific regions.

In order to achieve better design criteria, in the context of dynamic analysis of mechanical systems, it is of crucial importance to take into consideration the effects of wear in the geometrical changes on the mating surfaces of the different components. Also, from a tribological point of view, simulations like the one presented in this work can be a useful tool for the design process of any mechanical system as this approach can be used in predicting how a worn surface will affect the wear or, conversely, what characteristics should a material present to withstand a given set of working conditions.

Acknowledgments

The author would like to acknowledge the considerable contributions of Professor Kenneth Ludema from Michigan University, USA, Professor Alessandro Tasora from University of Parma, Italy, Professor Roberto Stefanelli from University of Rome Tor Vergata, Italy and Professor José Gomes from University of Minho, Portugal, for sharing with me some thoughts and ideas on the wear phenomenon in mechanical systems. Finally, I would also like to acknowledge the anonymous reviewers for their comments on an earlier draft of this paper.

References

[1] Gahr, K-H.Z., 1987, *Microstructure and wear of materials*. Amsterdam, Elsevier, p. 4.

[2] Meng, H.C., 1994, *Wear modelling: evaluation and categorization of wear models*. PhD Dissertation, University of Michigan, Ann Arbor, Michigan, USA.

[3] Meng, H.C., Ludema, K.C., 1995, "Wear models and predictive equations: their form and content". Wear, **181**-**183**, pp. 443-457.

[4] Stolarski, T.A., 1990, *Tribology in Machine Design*. Butterworth-Heinemann. Oxford, England.

[5] Hegadekatte, V., Huber, N., Kraft, O., 1975, "Finite element based simulation of dry sliding wear". Modeling and Simulation in Materials Science and Engineering, **13**, pp. 57-75.

[6] Yuksel, C., Kahraman, A., 2004, "Dynamic tooth loads of planetary gear sets having tooth profile wear". Mechanism and Machine Theory, **39**(7), pp. 695-715.

[7] Tasora, A., Prati, E., Silvestri, M., 2004, "Experimental investigation of clearance effects in a revolute joint". Proceedings of the 2004 AIMETA International Tribology Conference, Rome, Italy, September 14-17, 8p.

[8] Wojnarowski, J., Onishchenko, V., 2003, "Tooth wear effects on spur gear dynamics". Mechanism and Machine Theory, **38**(2), pp. 161-178.

[9] Reye, T., 1860, "Zur theorie der zapfengreibund". Der Civilingenieur, 4, pp. 235-255.

[10] Archard, J.F., 1953, "Contact and rubbing of flat surfaces". Journal of Applied Physics, **24**, pp. 981-988.

[11] Pennestri, E., Stefanelli, R., Valentini, P.P., Vita, L., 2004, "A dynamic simulation of cam actuated robotized gearbox". Proceedings of DETC'04 ASME Design Engineering Technical Conferences and Computers Information in Engineering Conference, Salt Lake City, Utah, USA, September 28-October 2, 12p.

[12] Põdra, P., Andersson, S., 1999, "Finite element analysis wear simulation of a conical spinning contact considering surface topology". Wear, **224**, pp. 13-21.

[13] Flodin, A., Andersson, S., 2000, "Simulation of mild wear in helicoidal gears". Wear, **241**, pp. 123-128.

[14] Nayak, N., Laksminarayanan, P.A., Badu, M.K.G., Dani, A.D., 2006, "Predictions of cam follower wear in diesel engines". Wear, **260**, pp. 181-192.

[15] Jourdan, F., 2006, "Numerical wear modeling in dynamics and large strains: Application to knee joint prostheses". Wear, **261**(3-4), pp. 283-292.

[16] Rabinowicz, E., 1995, *Friction and wear of materials*. Second edition, Wiley and Sons, New York.

[17] Nikravesh, P.E., 1988, *Computer-Aided Analysis of Mechanical Systems*, Prentice-Hall, Englewood Cliffs, New Jersey.

[18] Garcia de Jálon, J., Bayo, E., 1994, *Kinematic and Dynamic Simulations of Multibody Systems*. Springer Verlag, New York.

[19] Baumgarte, J., 1972, "Stabilization of Constraints and Integrals of Motion in Dynamical Systems", Computer Methods in Applied Mechanics and Engineering, **1**, pp. 1-16.

[20] Shampine, L., Gordon, M., 1975, *Computer Solution of Ordinary Differential Equations: The Initial Value Problem*. Freeman, San Francisco.

[21] Holm, R., 1946, *Electric contacts*. Almqvist & Wiksells Boktryckeri, Uppsala.

[22] Põdra, P., Andersson, S., 1997, "Wear simulation with the Winkler surface model". Wear, **207**(1-2), pp. 79-85.

[23] Lankarani, H. M., and Nikravesh, P. E., 1990, "A Contact Force Model With Hysteresis Damping for Impact Analysis of Multibody Systems". Journal of Mechanical Design, **112**, pp. 369-376.

[24] Ambrósio, J.A.C., 2002, "Impact of Rigid and Flexible Multibody Systems: Deformation Description and Contact Models", Virtual Nonlinear Multibody Systems, NATO, Advanced Study Institute, (edited by W. Schiehlen and M. Valásek), Vol. II, pp. 15-33.

[25] Flores, P., Ambrósio, J., Claro, J.C.P., Lankarani, H.M., Koshy, C.S., 2006, "A study on dynamics of mechanical systems including joints with clearance and lubrication". Mechanism and Machine Theory, **41**(3), pp. 247-261.

[26] Flores P, Ambrósio J., Claro J.P., 2004, "Dynamic Analysis for Planar Multibody Mechanical Systems with Lubricated Joints". Multibody System Dynamics, **12**, pp. 47-74.

[27] Karnopp, D., 1985, "Computer Simulation of Stick-Slid Friction in Mechanical Dynamic Systems". Journal of Dynamic Systems, Measurement, and Control, **107**, pp. 100-103.

[28] Centea, D., Rahnejat, H., Menday, M.T., 2001, "Non-linear multi-body dynamic analysis for the study of clutch torsional vibrations (judder)". Applied Mathematical Modelling, **25**, pp. 177-192.

[29] Haessig, D.A., Friedland, B., 1991, "On the Modelling and Simulation of Friction". Journal of Dynamic Systems, Measurement, and Control, **113**, pp. 354-362.

[30] Ahmed, S., Lankarani, H.M., Pereira, M.F.O.S., 1999, "Frictional Impact Analysis in Open Loop Multibody Mechanical System". Journal of Mechanical Design, **121**, pp. 119 127.

[31] Lankarani, H.M., 2000, "A Poisson Based Formulation For Frictional Impact Analysis of Multibody Mechanical Systems With Open or Closed Kinematic Chains". Journal of Mechanical Design, **115**, pp. 489-497.

[32] Gear, C.W., 1971, *Numerical Initial Value Problems in Ordinary Differential Equations*. Prentice-Hall, Englewood Cliffs, New Jersey.

[33] Ascher, U., Petzold, L., 1998, *Computer Methods for Ordinary Differential Equations and Differential-Algebraic Equations*. SIAM, Philadelphia.

[34] Flores, P., Ambrósio, J., Claro, J.C.P., Lankarani, H.M., 2008, *Kinematics and Dynamics of Multibody Systems with Imperfect Joints: Models and Case Studies*, Spinger Verlag, Berlin.

[35] Flores, P. Ambrósio, J., Claro, J.C.P., Lankarani, H.M., 2006, "Influence of the contact-impact force model on the dynamic response of multibody systems". Proceedings of the Institution of Mechanical Engineers, Part-K Journal of Multi-body Dynamics, **220**(1), pp. 21-34.

[36] Dubowsky, S., and Freudenstein, F., 1971, "Dynamic Analysis of Mechanical Systems With Clearances, Part 1: Formulation of Dynamic Model". Journal of Engineering for Industry, Series B, **93**(1), pp. 305-309.

[37] Dubowsky, S., and Freudenstein, F., 1971, "Dynamic Analysis of Mechanical Systems With Clearances, Part 2: Dynamic Response". Journal of Engineering for Industry, Series B, **93**(1), pp. 310-316.

[38] Dubowsky, S., and Gardner, T.N., 1977, "Design and Analysis of Multilink Flexible Mechanism With Multiple Clearance Connections". Journal of Engineering for Industry, Series B, **99**(1), pp. 88-96.

[39] Dubowsky, S., 1974, "On Predicting the Dynamic Effects of Clearances in Planar Mechanisms". Journal of Engineering for Industry, Series B, **96**(1), pp. 317-323.

[40] Winfrey, R.C., Anderson, R.V., and Gnilka, C.W., 1973, "Analysis of Elastic Machinery With Clearances". Journal of Engineers for Industry, **95**, pp. 695-703.

[41] Bauchau, O.A., and Rodriguez, J., 2002, "Modelling of Joints with Clearance in Flexible Multibody Systems". International Journal of Solids and Structures, **39**, pp. 41-63.

[42] Dubowsky, S., and Moening, M.F., 1978, "An Experimental and Analytical Study of Impact Forces in Elastic Mechanical Systems with Clearances". Mechanism and Machine Theory, **13**, pp. 451-465.